Supplemental Material: State-dependent optical lattices for the strontium optical qubit

A. Heinz,[1,2,*] A. J. Park,[1,2,*] N. Šantić,[1,2] J. Trautmann,[1,2] S. G. Porsev,[3,4] M. S. Safronova,[3,5] I. Bloch,[1,2,6] and S. Blatt[1,2,†]

[1]*Max-Planck-Institut für Quantenoptik, Hans-Kopfermann-Straße 1, 85748 Garching, Germany*
[2]*Munich Center for Quantum Science and Technology, 80799 München, Germany*
[3]*Department of Physics and Astronomy, University of Delaware, Newark, Delaware 19716, USA*
[4]*Petersburg Nuclear Physics Institute of NRC "Kurchatov Institute," Gatchina, Leningrad district 188300, Russia*
[5]*Joint Quantum Institute, National Institute of Standards and Technology and the University of Maryland, College Park, Maryland, 20742, USA*
[6]*Fakultät für Physik, Ludwig-Maximilians-Universität München, 80799 München, Germany*

(Dated: May 2, 2020)

I. PARAMETRIC HEATING IN INCOMMENSURATE LATTICES

The optical dipole potential of two retroreflected laser beams with different wavelengths $\lambda_i = 2\pi/k_i$ along the z-direction is

$$u(z) = u_1 \cos^2(k_1 z) + u_2(t) \cos^2(k_2 z). \tag{S1}$$

Here u_i is the lattice depth induced on the atomic state via the AC Stark effect. In the parametric-heating experiments described in the main text, the first lattice is the deep magic-wavelength lattice with a fixed depth u_1. The second lattice is the shallow tune-out lattice with a variable depth $u_2(t) = u_2^0 + u_2^{\mathrm{mod}} \cos(\omega_{\mathrm{mod}} t)$ that is sinusoidally modulated around its mean value u_2^0 with a modulation amplitude u_2^{mod} and a modulation frequency ω_{mod}. Since we use shallow tune-out lattices with $u_2(t) \ll u_1$, we treat the effect of the shallow lattice in perturbation theory by expressing its effect as a variation in the trap position and the trap frequency of each lattice site [S1–S3]. To this end, we expand the combined lattice potential around the position $z_j = (2j+1)\pi/(2k_1)$ of the j-th minimum of the deep lattice and find

$$\begin{aligned} u(z) \approx\ & u_2(t) \cos^2(k_2 z_j) - u_2(t) \sin(2k_2 z_j) k_2 (z - z_j) \\ & + [u_1 k_1^2 - u_2(t) k_2^2 \cos(2k_2 z_j)](z - z_j)^2. \end{aligned} \tag{S2}$$

By completing the squares and dropping constant terms, we can bring the above expression into the standard form [S1–S3] for parametric heating in a harmonic oscillator

$$u \approx \frac{m\omega_j^2}{2}(1+\epsilon)[z - (\tilde{z}_j + \delta_j)]^2, \tag{S3}$$

where m is the mass of the atom, ω_j ($\tilde{z}_j$) is the unmodulated trap frequency (position of the minimum) of lattice site j, and ϵ (δ_j) is the amplitude (position) modulation causing transitions between the harmonic oscillator levels. Explicitly, we find

$$\begin{aligned} m\omega_j^2/2 &= u_1 k_1^2 - u_2^0 k_2^2 \cos 2k_2 z_j, \\ \epsilon &= \frac{u_2^{\mathrm{mod}}}{u_1} \cos \omega_{\mathrm{mod}} t, \\ \tilde{z}_j &= z_j - \left(\frac{k_2}{2k_1^2} \sin 2k_2 z_j \right) \frac{u_2^0}{u_1}, \\ \delta_j &= \left(\frac{k_2}{2k_1^2} \sin 2k_2 z_j \right) \frac{u_2^{\mathrm{mod}}}{u_1} \cos \omega_{\mathrm{mod}} t. \end{aligned} \tag{S4}$$

From these expressions we see that the trap frequency of the deep lattice $m\omega_1^2/2 = u_1 k_1^2$ is very weakly influenced by the presence of a weak lattice with bare trap frequency $m\omega_2^2/2 = u_2^0 k_2^2$. These trap frequencies scale with the ratio of the ground state polarazibilites $\alpha_g(\lambda_i)$ at the magic and tune-out wavelengths and the lattice powers P_i. For our parameters, we find

$$\frac{\omega_2^2}{\omega_1^2} \propto \frac{\alpha_g(\lambda_2) P_2}{\alpha_g(\lambda_1) P_1} \simeq 5 \times 10^{-5}. \tag{S5}$$

For this reason, the trap frequency of the combined lattice is unchanged when modulating the deep lattice by itself or when modulating the shallow lattice in the presence of the deep lattice. In the latter case, the modulation spectrum simply acquires a second minimum at the trap frequency, corresponding to position modulation of the lattice sites.

II. TRAP LOSS FITTING

To analyze the trap loss curves throughout the main text, we fit the atom number data $N(t)$ as a function of time t with exponential decay curves $N(t) = N_0 e^{-\Gamma t}$ resulting from a single-body decay process $\dot{N} = -\Gamma N$. We decide whether to fit with superexponential decay

$$N(t) = N_0 \frac{\Gamma e^{-\Gamma t}}{\Gamma + N_0 b (1 - e^{-\Gamma t})}, \tag{S6}$$

due to an additional two-body decay process $\dot{N} = -\Gamma N - bN^2$ based on a χ^2 test. This two-body loss model assumes a homogeneous density in the trap that attenuates

homogeneously without changing the sample temperature. Because we do not take the temperature effects of evaporation and anti-evaporation into account, the results of the superexponential decay curves are *not* used to derive any of the important quantities in the main text and are meant simply as a guide to the eye.

III. TRAP LOSS RATE RESCALING

If we modulate with $\omega_{\rm mod} = 2\pi f_{\rm mod} = 2\omega_1$ (at twice the deep lattice trap frequency), the differential trap loss rate is proportional to the heating rate caused by the intensity modulation alone [S1–S3]

$$\begin{aligned}\Gamma_{\rm mod} &\propto f_{\rm mod}^2 S_\epsilon(f_{\rm mod}) \\ &\propto \omega_1^2 \left(\frac{u_2^{\rm mod}}{u_1}\right)^2 \end{aligned} \tag{S7}$$

where $S_\epsilon(f_{\rm mod})$ is the power spectrum of the fractional intensity noise at the modulation frequency $f_{\rm mod} = \omega_{\rm mod}/2\pi$. The ratio of shallow modulation amplitude to deep lattice trap depth, $u_2^{\rm mod}/u_1 = \alpha_g(\lambda_2) I_{\rm mod}/[\alpha_g(\lambda_1) I_1]$ where $I_{\rm mod}$ is the intensity modulation amplitude of the shallow lattice and I_1 is the intensity of the deep lattice. Thus,

$$\Gamma_{\rm mod} \propto \alpha_g(\lambda_2)^2 f_{\rm mod}^2 \left(\frac{I_{\rm mod}}{I_1}\right)^2 \propto \alpha_g(\lambda_2)^2 \frac{I_{\rm mod}^2}{f_{\rm mod}^2}, \tag{S8}$$

where we have used $I_1 \propto \omega_1^2 \propto f_{\rm mod}^2$. To compensate for possible experimental variations in ω_1 and $I_{\rm mod}$, we scale the measured induced loss rate with respect to the reference values

$$\Gamma_{\rm mod}^{\rm scaled} = \Gamma_{\rm mod} \left(\frac{f_{\rm mod}}{f_{\rm mod}^{\rm ref}}\right)^2 \left(\frac{I_{\rm mod}^{\rm ref}}{I_{\rm mod}}\right)^2, \tag{S9}$$

and work with these scaled induced loss rates throughout the main text.

IV. THE ^{1}S$_0$ GROUND STATE TUNE-OUT WAVELENGTH

The polarizability of an electronic state consists of contributions from the core electrons and valence electrons. The valence part of the ground state ^{1}S$_0$ (g) polarizability is determined by summing over all the contributions of excited states dipole-coupled to g, dominated by the ^{1}P$_1$ and ^{3}P$_1$ contributions. For this reason, we write the g polarizability using the four components

$$\alpha_g(\omega) = \alpha_g(^1{\rm P}_1;\omega) + \alpha_g(^3{\rm P}_1;\omega) + \alpha_g(v;\omega) + \alpha_g(c;\omega), \tag{S10}$$

where $\alpha_g(j;\omega)$ are the contributions from the excited state j, $\alpha_g(v;\omega)$ is the sum of contributions from all other valence states, $\alpha_g(c;\omega)$ is the contribution of the core electrons, and $\omega = 2\pi c/\lambda$ is the optical frequency for wavelength λ.

The contribution from the ^{1}P$_1$ and ^{3}P$_1$ states further splits into scalar, vector, and tensor components as [S4, S5]

$$\begin{aligned}\alpha_g(j;\omega) = &\alpha_g^s(j;\omega) \\ &+ \alpha_g^v(j;\omega)(i\boldsymbol{\epsilon}\times\boldsymbol{\epsilon}^*)\cdot\boldsymbol{e}_z \frac{m_F}{F} \\ &+ \alpha_g^t(j;\omega)\frac{3|\boldsymbol{\epsilon}\cdot\boldsymbol{e}_z|^2 - 1}{2}\frac{3m_F^2 - F(F+1)}{F(2F-1)},\end{aligned} \tag{S11}$$

where F is the hyperfine quantum number associated with the ground state g, m_F is the corresponding magnetic quantum number, and j indicates one of the excited states ^{1}P$_1$ and ^{3}P$_1$. The ^{1}S$_0$ (g) state of the fermionic isotope ^{87}Sr has a single hyperfine state $F = 9/2$, since the electronic angular momentum J and the nuclear spin I are 0 and 9/2, respectively ($|J - I| \le F \le |J + I|$). For the bosonic isotope ^{88}Sr where $I = 0$, J replaces F ($F = J$). Therefore, any discussion involving F_j throughout this text only applies to ^{87}Sr. The quantization axis is assumed to be along $\boldsymbol{e}_z$, and $\boldsymbol{\epsilon}$ is the complex polarization vector of the applied laser at frequency ω. The vector and tensor components depend on the polarization of the applied beam, while the scalar component does not.

The scalar, vector, and tensor parts themselves can be written as sums over all hyperfine states F_j in the excited fine structure state [S4, S5]

$$\begin{aligned}\alpha_g^s(j;\omega) &= \sum_{F_j} \frac{2}{3} g_{j,F_j}^{(0)}(\omega)|D_{j,F_j}|^2, \\ \alpha_g^v(j;\omega) &= \sum_{F_j} (-1)^{F+F_j+1}\sqrt{\frac{6F(2F+1)}{F+1}} \\ &\qquad \times \begin{Bmatrix} 1 & 1 & 1 \\ F & F & F_j \end{Bmatrix} g_{j,F_j}^{(1)}(\omega)|D_{j,F_j}|^2, \\ \alpha_g^t(j;\omega) &= \sum_{F_j} (-1)^{F+F_j}\sqrt{\frac{40F(2F-1)(2F+1)}{3(F+1)(2F+3)}} \\ &\qquad \times \begin{Bmatrix} 1 & 1 & 2 \\ F & F & F_j \end{Bmatrix} g_{j,F_j}^{(2)}(\omega)|D_{j,F_j}|^2.\end{aligned} \tag{S12}$$

Scaling of the polarizability terms as a function of laser detuning is encapsulated in the detuning factors

$$\begin{aligned} g_{j,F_j}^{(K)}(\omega) &= \frac{1}{2\hbar}{\rm Re}\left(\frac{1}{\omega_{j,F_j} - \omega - \frac{i}{2\tau_j}} + \frac{(-1)^K}{\omega_{j,F_j} + \omega + \frac{i}{2\tau_j}}\right) \\ &\approx \frac{1}{2\hbar}\left(\frac{1}{\omega_{j,F_j} - \omega} + \frac{(-1)^K}{\omega_{j,F_j} + \omega}\right)\end{aligned} \tag{S13}$$

where ω_{j,F_j} is the transition frequency from the ground to the excited hyperfine state F_j, τ_j is the excited state lifetime, and $K = 0$, 1, 2 for scalar, vector, and tensor polarizabilities, respectively [S4, S5]. Because we work in the far-detuned regime, we can ignore the imaginary

terms in the denominators of Eqn. (S13), which we have confirmed numerically. The detuning factor is identical for the scalar and tensor polarizabilities, but the counter-rotating term for the vector polarizability changes its sign. Note that ω_{j,F_j} can be expressed in terms of the (hypothetical) hyperfine-free transition frequency $\bar{\omega}_j$ and the hyperfine shift Δ_{j,F_j} as $\omega_{j,F_j} = \bar{\omega}_j + \Delta_{j,F_j}$. The hyperfine shift can be calculated from the magnetic dipole interaction constant A_j and the electric quadrupole interaction constant Q_j as [S6, S7]

$$\Delta_{j,F_j} = \frac{A_j}{2}K_j + \frac{Q_j}{4}\frac{\frac{3}{2}K_j(K_j+1) - 2I(I+1)J_j(J_j+1)}{I(2I-1)J_j(2J_j-1)}, \\ K_j = F_j(F_j+1) - J_j(J_j+1) - I(I+1), \tag{S14}$$

where J_j is the electronic angular momentum of the excited state. We use the hyperfine constants $A_{^1\mathrm{P}_1} = -2\pi \times 3.4(4)$ MHz, $Q_{^1\mathrm{P}_1} = 2\pi \times 39(4)$ MHz, $A_{^3\mathrm{P}_1} = -2\pi \times 260.084(2)$ MHz, and $Q_{^3\mathrm{P}_1} = -2\pi \times 35.658(6)$ MHz, summarized in Ref. [S6]. The isotope shift of $\bar{\omega}_{^3\mathrm{P}_1}$ was measured recently in Ref. [S8]: the hyperfine-free transition frequency of $^1\mathrm{S}_0$-$^3\mathrm{P}_1$ in ^{87}Sr is red detuned by 62.1865(123) MHz from the transition frequency in ^{88}Sr, 434,829,121,311(10) kHz [S9]. The $^1\mathrm{S}_0$-$^1\mathrm{P}_1$ transition frequency does not need to be as precise and is obtained from Ref. [S10]. The isotope shift on this transition does not influence the calculations, as will be shown below.

All polarizability terms scale with the modulus-squared of the reduced matrix element associated with the corresponding dipole transition

$$|D_{j,F_j}|^2 = |\langle g, F \| D \| j, F_j \rangle|^2. \tag{S15}$$

Since the $^1\mathrm{S}_0$ state of ^{87}Sr has a single hyperfine state, the reduced matrix element can be expressed in terms of the excited state lifetime τ_j as

$$|D_{j,F_j}|^2 = \frac{3\pi\epsilon_0\hbar c^3}{\omega_{j,F_j}^3\tau_j}(2J_j+1)(2F_j+1)\begin{Bmatrix} J & J_j & 1 \\ F_j & F & I \end{Bmatrix}^2. \tag{S16}$$

The two excited states of interest $^1\mathrm{P}_1$ and $^3\mathrm{P}_1$ both have $J_j = 1$, and thus have the same three hyperfine states $F_j = 7/2$, $9/2$, and $11/2$. For this reason, the scalar, vector, and tensor polarizabilities only differ in the group-theoretic numerical prefactors associated with the excited states, except for the slightly different detuning dependence of the vector polarizability.

The situation simplifies strongly for the case of ^{88}Sr. If we replace F (F_j) with J (J_j) in Eqn. (S12), the vector and tensor polarizabilities vanish. Only the scalar component remains in the absence of hyperfine structure.

To study the contributions from each component in detail, we dig deeper into the scalar, vector, and tensor polarizabilities of the ^{87}Sr $^1\mathrm{S}_0$ state. By specializing the prefactors, we re-write the reduced matrix elements as

$$|D_{j,F_j}|^2 = \frac{3\pi\epsilon_0\hbar c^3}{\omega_{j,F_j}^3\tau_j}\{4/5, 1, 6/5\}, \tag{S17}$$

where the numerical factors in the braces correspond to $F_j = 7/2$, $9/2$, and $11/2$, respectively. As expected, this means that the lifetime τ proportionally scales up scalar, vector, and tensor polarizabilities. Bringing it all together, we find

$$\alpha_g^s(j;\omega) = 2\sum_{F_j}\frac{3\pi\epsilon_0\hbar c^3}{\omega_{j,F_j}^3\tau_j}\left\{\frac{4}{15}, \frac{5}{15}, \frac{6}{15}\right\} g_{j,F_j}^{(0)}(\omega), \\ \alpha_g^v(j;\omega) = \sum_{F_j}\frac{3\pi\epsilon_0\hbar c^3}{\omega_{j,F_j}^3\tau_j}\left\{-\frac{44}{55}, -\frac{10}{55}, \frac{54}{55}\right\} g_{j,F_j}^{(1)}(\omega), \\ \alpha_g^t(j;\omega) = \frac{\sqrt{2}}{3}\sum_{F_j}\frac{3\pi\epsilon_0\hbar c^3}{\omega_{j,F_j}^3\tau_j}\left\{-\frac{88}{165}, \frac{160}{165}, -\frac{72}{165}\right\} g_{j,F_j}^{(2)}(\omega). \tag{S18}$$

To get an intuitive picture of what happens in the far-detuned regime compared to the hyperfine structure, we approximate $|D_{j,F_j}|^2 \approx \frac{3\pi\epsilon_0\hbar c^3}{\bar{\omega}_j^3\tau_j}\{4/5, 1, 6/5\}$ to pull $\frac{3\pi\epsilon_0\hbar c^3}{\omega_{j,F_j}^3\tau_j}$ out of the sum in Eqn. (S18). After this approximation, we see that both vector and tensor polarizabilities sum to zero when we are in the far-detuned regime compared to the hyperfine structure, where the detuning factor contributes equally, and can be pulled out of the sum. In this regime, the only contribution that survives is the scalar polarizability. For the same reason, we also expect negligible differences in α^s between the two isotopes in this regime. The scalar polarizabilities of the two isotopes are illustrated in Fig. S1(a) where we see that they become indistinguishable as the detuning from the $^1\mathrm{S}_0$-$^3\mathrm{P}_1$ transition increases (the plot was generated based on Eqn. (S18) without the approximation on $|D_{j,F_j}|^2$). Note that the detuning for ^{87}Sr is referenced with respect to $\bar{\omega}_j$, which takes the isotope shift into account.

Next, we take a closer look at each contribution in the detuning range relevant to our experimental data. Comparing Fig. S1(b)-(c) and (e)-(f), the $^1\mathrm{P}_1$ tensor and vector contributions are more than two orders of magnitude smaller than the contributions from the $^3\mathrm{P}_1$ state, since the frequency of the shallow lattice is more than a few hundred THz detuned from the $^1\mathrm{S}_0$-$^1\mathrm{P}_1$ transition. For this reason, we can ignore the vector and tensor contributions to $\alpha_g(^1\mathrm{P}_1;\omega)$ and set $\alpha_g(^1\mathrm{P}_1;\omega) = \alpha_g^s(^1\mathrm{P}_1;\omega)$.

With this simplification, we analyze the difference of the ^{87}Sr and ^{88}Sr tune-out detuning Δ_t due to the hyperfine structure. At the tune-out detuning, $\alpha_g(^1\mathrm{P}_1;\omega)$ balances $\alpha_g(^3\mathrm{P}_1;\omega)$ and the remaining valence and core contributions to the polarizability, $\alpha_{\mathrm{vc}} = \alpha_g(v;\omega) + \alpha_g(c;\omega)$.

We calculated the valence part of α_g by solving the inhomogeneous equation as described in Refs. [S11, S12]. Then, using the sum-over-states formula Eqn. (S12), we extracted the contributions of the $^1\mathrm{P}_1$ and $^3\mathrm{P}_1$ states and determined the remaining valence contributions, $\alpha_g(v, \Delta_t) = 6.57(14)$ a.u. The core part of the polarizability, $\alpha_g(c;\Delta_t)$, was calculated in the single-electron approximation including random-phase approximation corrections [S13] to be $\alpha_g(c;\Delta_t) = 5.30(5)$ a.u.

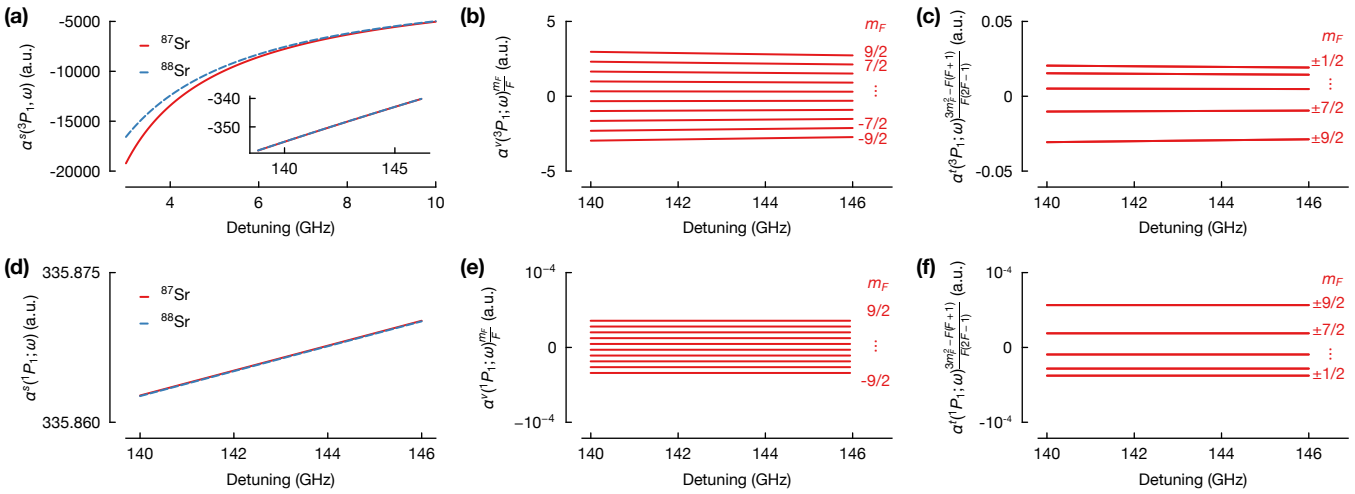

FIG. S1. (color online). (a) The ^{3}P$_1$ scalar contribution as a function of detuning from the ^{1}S$_0$-^{3}P$_1$ transition. For the case of ^{87}Sr, the detuning is referenced with respect to $\bar{\omega}_{^3\mathrm{P}_1}$, which includes the isotope shift. The inset shows $\alpha^s_{^3\mathrm{P}_1}$ at the detuning range relevant to our data. (b) the ^{3}P$_1$ vector contribution as a function of detuning from the ^{1}S$_0$-^{3}P$_1$ transition for different m_F states (Eqn. (S12)). We assume the beam ellipticity of 1 to show the upper limit. (c) the ^{3}P$_1$ tensor contribution (Eqn. (S12)) as a function of detuning from the ^{1}S$_0$-^{3}P$_1$ transition for different m_F states. Here, we assume a linear polarization to show the upper limit. (c)-(f) same as (a)-(c), but from the ^{1}P$_1$ contributions.

$\alpha_g(^3\mathrm{P}_1,\omega)$	$\delta\Delta_t = \Delta_t^{87} - \Delta_t^{88}$
$\alpha_g^s(^3\mathrm{P}_1;\omega)$	$+2\pi \times 8$ MHz
$\alpha_g^v(^3\mathrm{P}_1;\omega)$	$-2\pi \times 23$ MHz $\leq \delta\Delta_t \leq +2\pi \times 23$ MHz
$\alpha_g^t(^3\mathrm{P}_1;\omega)$	$-2\pi \times 2$ MHz $\leq \delta\Delta_t \leq +2\pi \times 12$ MHz

TABLE I. Comparison of the ^{87}Sr and ^{88}Sr tune-out detuning: Δ_t^{87} was numerically computed considering the contributions shown in the left column. For the vector and tensor contributions, the shift was calculated for the stretched $|m_F| = F$ states and we show the corresponding ranges. A beam ellipticity of 2% was used for the vector shifts and we assumed perfect (maximum) polarization alignment for the tensor shifts.

Table I shows the shifts due to scalar, vector, and tensor polarizabilities. For the calculations due to the vector polarizabilities, we used an upper limit on the beam ellipticity of 2%, measured by a polarimeter after transmission through our vacuum chamber, and assumed perfect alignment of $\boldsymbol{\epsilon}\cdot\boldsymbol{e}_z = 1$ to evaluate the tensor polarizability. The shifts depend on the m_F states (Eqn. (S12)), and we show the maximum ranges of the shift as a worst case estimate. In the experiment, we do not spin-polarize the sample, and we likely work with an equal population among all m_F states. As a conservative estimate, we use the full span due to the vector shift to estimate differential shifts between the measured tune-out detuning Δ_t^{88} for ^{88}Sr and the tune-out detuning Δ_t^{87} for ^{87}Sr. By choosing to work with Δ_t^{88}, we thus estimate a mismatch of ± 23 MHz, corresponding to a residual ground state polarizability of ± 0.05 a.u. for the AC Stark shift measurements presented in the main text.

Putting everything together, the scalar parts can be explicitly written as

$$\alpha_g^s(^3\mathrm{P}_1;\omega) = \frac{6\pi\epsilon_0 c^3}{\bar{\omega}^3_{^3\mathrm{P}_1}\tau_{^3\mathrm{P}_1}} \sum_{F_j} \left\{\frac{4}{15}, \frac{5}{15}, \frac{6}{15}\right\} \frac{\omega_{^3\mathrm{P}_1,F_{^3\mathrm{P}_1}}}{\omega^2_{^3\mathrm{P}_1,F_{^3\mathrm{P}_1}} - \omega^2},$$
$$\alpha_g^s(^1\mathrm{P}_1;\omega) \approx \frac{6\pi\epsilon_0 c^3}{\tau_{^1\mathrm{P}_1}\omega^2_{^1\mathrm{P}_1}(\omega^2_{^1\mathrm{P}_1} - \omega^2)}, \tag{S19}$$

where we have neglected the hyperfine splitting in $\alpha_g^s(^1\mathrm{P}_1;\omega)$. These approximations result in an additional shift of Δ_t by a few hundred kHz, which is more than two orders of magnitude smaller than our experimental precision. As a consequence, we can express $\tau_{^1\mathrm{P}_1}$ directly in terms of the tune-out frequency

$$\tau_{^1\mathrm{P}_1} = \frac{-6\pi\epsilon_0 c^3}{[\alpha_g(v;\omega_t) + \alpha_g(c;\omega_t) + \alpha_g^s(^3\mathrm{P}_1,\omega_t)]\omega^2_{^1\mathrm{P}_1}(\omega^2_{^1\mathrm{P}_1} - \omega_t^2)} \tag{S20}$$

For ^{88}Sr, where the ^{3}P$_1$ hyperfine splittings are absent, no approximations are necessary. Thus, $\alpha_g^s(^3\mathrm{P}_1,\omega_t)$ reduces to

$$\alpha_g^s(^3\mathrm{P}_1;\omega_t) = \frac{6\pi\epsilon_0 c^3}{\tau_{^3\mathrm{P}_1}\omega^2_{^3\mathrm{P}_1}(\omega^2_{^3\mathrm{P}_1} - \omega_t^2)}. \tag{S21}$$

To derive a fitting function to model the induced loss rate $\Gamma_{\mathrm{mod}} \propto (\alpha_g^s)^2$, we first need to express $g^{(0)}_{^3\mathrm{P}_1,F_{^3\mathrm{P}_1}}$ explicitly

in terms of the laser detuning $\Delta = \omega - \bar{\omega}_{^3\mathrm{P}_1}$,

$$\begin{aligned} g^{(0)}_{^3\mathrm{P}_1,F_{^3\mathrm{P}_1}}(\omega) &= \frac{1}{\hbar}\frac{\omega_{^3\mathrm{P}_1,F_{^3\mathrm{P}_1}}}{\omega^2_{^3\mathrm{P}_1,F_{^3\mathrm{P}_1}} - \omega^2} \\ &= \frac{1}{2\hbar}\left(\frac{1}{\omega_{^3\mathrm{P}_1,F_{^3\mathrm{P}_1}} - \omega} + \frac{1}{\omega_{^3\mathrm{P}_1,F_{^3\mathrm{P}_1}} + \omega}\right) \\ &\approx \frac{1}{2\hbar}\left(\frac{1}{\Delta_{^3\mathrm{P}_1,F_{^3\mathrm{P}_1}} - \Delta} + \frac{1}{2\bar{\omega}_{^3\mathrm{P}_1}}\right), \end{aligned} \tag{S22}$$

where we use $\omega_{j,F_j} = \bar{\omega}_j + \Delta_{j,F_j}$ and $2\bar{\omega}_{^3\mathrm{P}_1} \gg \Delta + \Delta_{^3\mathrm{P}_1,F_{^3\mathrm{P}_1}}$. For the case of ^{88}Sr, $\bar{\omega}_j$ is replaced by ω_j. The last approximation on $g^{(0)}_{^3\mathrm{P}_1}$ shifts Δ_t by only several kHz. Then, $\alpha^s_g(j;\omega)$ can be written as a function of the detuning as

$$\begin{aligned} \alpha^s_g(^3\mathrm{P}_1;\Delta) \approx \frac{1}{\tau_{^3\mathrm{P}_1}}\frac{3\pi\epsilon_0 c^3}{2\bar{\omega}^4_{^3\mathrm{P}_1}}\Bigg[1- \\ 2\sum_{F_{^3\mathrm{P}_1}}\left\{\frac{4}{15},\frac{5}{15},\frac{6}{15}\right\}\frac{\bar{\omega}_{^3\mathrm{P}_1}}{\Delta - \Delta_{^3\mathrm{P}_1,F_{^3\mathrm{P}_1}}}\Bigg]. \end{aligned} \tag{S23}$$

From this equation, we see that $\alpha^s_g(^3\mathrm{P}_1;\Delta)$ scales inversely proportional to detuning. As shown in Fig. S1(c), $\alpha^s_g(^1\mathrm{P}_1;\Delta)$ varies at the 10^{-3} level in the detuning range of our experimental data. Thus, we treat $\alpha^s_g(^1\mathrm{P}_1;\Delta)$ as a constant $\alpha^s_g(^1\mathrm{P}_1;\Delta) = \alpha^s_g(^1\mathrm{P}_1;\Delta_t)$, which shifts Δ_t by less than a kHz. Focusing on ^{88}Sr where the hyperfine structure is absent, we arrive at the following expression when treating α_{bg} also as a constant in the vicinity of Δ_t,

$$\alpha_g(\Delta_{^3\mathrm{P}_1}) = \mathrm{const} \times \left(1 - \frac{\Delta_t}{\Delta}\right). \tag{S24}$$

where we used the fact that α_g vanishes at the tune-out wavelength. We use the function above to fit the induced loss rates, $\Gamma_{\mathrm{mod}} \propto \alpha^2_g(\Delta_{^3\mathrm{P}_1})$.

V. FOURIER FILTERING

To suppress amplified spontaneous emission (ASE) that would induce systematic shifts in our measurements we took great care in filtering it. Of particular importance is the amount of ASE near the ^{1}S$_0$-^{3}P$_1$ transition where the polarizability diverges. Even very low light levels near this transition lower the lifetime of atoms in the magic wavelength lattice and introduce an uncontrolled heating mechanism that is not easily accounted for.

To minimize the amount of light away from the carrier, we Fourier filter the tune-out laser beam with a grating as the dispersive element. We expand the beam to a $1/e^2$ waist of 2 cm and diffract it from a holographic grating with 2400 lines/mm, propagate it over ∼6 m, before finally coupling it into a single-mode polarization-maintaining fiber.

We determine the achieved resolution by measuring the transmission through the fiber while changing the input wavelength, at the same time keeping the grating angle fixed. The Gaussian suppression line shape has a FWHM of 13 GHz, giving a suppression of more than 40 dB at the ^{1}S$_0$-^{3}P$_1$ frequency when the input light is at the tune-out frequency. Before filtering, we measure an ASE level of −50 dB compared to the carrier with a spectrum analyzer with a 0.05 nm resolution. Together with the achieved Fourier filtering suppression of 40 dB we conclude that the ASE level is reduced to below −90 dB compared to the carrier.

VI. LOADING EXCITED STATE ATOMS IN THE TUNE-OUT LATTICE

To load excited state ^{87}Sr atoms into the tune-out lattice the experimental procedure is as follows. We (i) load a sample of ^{87}Sr g atoms into the magic wavelength lattice; (ii) after 50 ms, we transfer ∼70% of the atoms to e using a 10-ms-long adiabatic-rapid-passage pulse; (iii) after another 2 ms, we diabatically switch on the tune-out lattice using 64 mW of power; (iv) after an additional 1 ms, we ramp down the magic wavelength lattice over 10 ms and retain ∼80% of the e atoms in the tune-out lattice; (v) we hold the atoms in the tune-out lattice for a given time, diabatically turn it off, repump the atoms to g over 2 ms [S14], and take an absorption image to determine the final atom number. In addition to matching the trapping frequencies of the tune-out and magic wavelength lattices, care was taken to achieve good mode matching between the two lattice beams. As a result the size and position of the area occupied by the trapped e atoms in the tune-out and the magic lattice differs on the single micron level. This is also supported by a measured moderate increase of the atom temperature to 3 μK after the transfer into the tune-out lattice.

* A. H. and A. J. P. contributed equally to this work.
† sebastian.blatt@mpq.mpg.de

[S1] T. A. Savard, K. M. O'Hara, and J. E. Thomas, Laser-noise-induced heating in far-off resonance optical traps, Phys. Rev. A **56**, R1095 (1997).
[S2] M. Gehm, K. O'Hara, T. Savard, and J. Thomas, Dynamics of noise-induced heating in atom traps, Phys. Rev. A **58**, 3914 (1998).
[S3] M. Gehm, K. O'Hara, T. Savard, and J. Thomas, Erratum: Dynamics of noise-induced heating in atom traps

[Phys. Rev. A 58, 3914 (1998)], Phys. Rev. A **61**, 029902 (2000).

[S4] N. L. Manakov, V. D. Ovsiannikov, and L. P. Rapoport, Atoms in a laser field, Phys. Rep. **141**, 320 (1986).

[S5] F. L. Kien, P. Schneeweiss, and A. Rauschenbeutel, Dynamical polarizability of atoms in arbitrary light fields: general theory and application to cesium, Eur. Phys. J. D **67**, 92 (2013).

[S6] M. M. Boyd, *High Precision Spectroscopy of Strontium in an Optical Lattice: Towards a New Standard for Frequency and Time*, Ph.D. thesis, University of Colorado, Department of Physics (2007).

[S7] M. Boyd, T. Zelevinsky, A. Ludlow, S. Blatt, T. Zanon-Willette, S. Foreman, and J. Ye, Nuclear spin effects in optical lattice clocks, Phys. Rev. A **76**, 022510 (2007).

[S8] H. Miyake, N. C. Pisenti, P. K. Elgee, A. Sitaram, and G. K. Campbell, Isotope shift spectroscopy of the $^1S_0 \rightarrow {}^3P_1$ and $^1S_0 \rightarrow {}^3P_0$ transitions in strontium, Phys. Rev. Research **1**, 033113 (2019).

[S9] G. Ferrari, P. Cancio, R. Drullinger, G. Giusfredi, N. Poli, M. Prevedelli, C. Toninelli, and G. M. Tino, Precision frequency measurement of visible intercombination lines of strontium, Phys. Rev. Lett. **91**, 243002 (2003).

[S10] J. E. Sansonetti and G. Nave, Wavelengths, transition probabilities, and energy levels for the spectrum of neutral strontium (Sr I), J. Phys. Chem. Ref. Data **39**, 033103 (2010).

[S11] M. G. Kozlov and S. G. Porsev, Polarizabilities and hyperfine structure constants of the low-lying levels of barium, Eur. Phys. J. D **5**, 59 (1999).

[S12] M. S. Safronova, S. G. Porsev, U. I. Safronova, M. G. Kozlov, and C. W. Clark, Blackbody-radiation shift in the Sr optical atomic clock, Phys. Rev. A **87**, 012509 (2013).

[S13] M. S. Safronova, W. R. Johnson, and A. Derevianko, Relativistic many-body calculations of energy levels, hyperfine constants, electric-dipole matrix elements, and static polarizabilities for alkali-metal atoms, Phys. Rev. A **60**, 4476 (1999).

[S14] S. Snigirev, A. J. Park, A. Heinz, I. Bloch, and S. Blatt, Fast and dense magneto-optical traps for strontium, Phys. Rev. A **99**, 063421 (2019).